

# Signal Transduction Cross Talk Mediated by Jun N-Terminal Kinase-Interacting Protein and Insulin Receptor Substrate Scaffold Protein Complexes<sup>∇</sup>

Claire L. Standen,<sup>1</sup> Norman J. Kennedy,<sup>1</sup> Richard A. Flavell,<sup>2</sup> and Roger J. Davis<sup>1\*</sup>

Howard Hughes Medical Institute and Program in Molecular Medicine, University of Massachusetts Medical School, Worcester, Massachusetts 01605,<sup>1</sup> and Howard Hughes Medical Institute and Section of Immunobiology, Yale University School of Medicine, Yale University, New Haven, Connecticut 06520<sup>2</sup>

Received 3 February 2009/Returned for modification 16 March 2009/Accepted 23 June 2009

**Scaffold proteins have been established as important mediators of signal transduction specificity. The insulin receptor substrate (IRS) proteins represent a critical group of scaffold proteins that are required for signal transduction by the insulin receptor, including the activation of phosphatidylinositol 3 kinase. The c-Jun NH<sub>2</sub>-terminal kinase (JNK)-interacting proteins (JIPs) represent a different group of scaffold molecules that are implicated in the regulation of the JNK. These two signaling pathways are functionally linked because JNK can phosphorylate IRS1 on the negative regulatory site Ser-307. Here we demonstrate the physical association of these signaling pathways using a proteomic approach that identified insulin-regulated complexes of JIPs together with IRS scaffold proteins. Studies using mice with JIP scaffold protein defects confirm that the JIP1 and JIP2 proteins are required for normal glucose homeostasis. Together, these observations demonstrate that JIP proteins can influence insulin-stimulated signal transduction mediated by IRS proteins.**

The c-Jun NH<sub>2</sub>-terminal kinase (JNK)-interacting proteins (JIPs) are implicated in the regulation of the JNK signal transduction pathway (8, 28). The JIP1 and JIP2 proteins are structurally related with similar modular domains (SH3 and PTB) and binding sites for the mixed-lineage protein kinase (MLK) group of mitogen-activated protein kinase (MAPK) kinase kinases, the MAPK kinase MKK7, and JNK (19). These JIP proteins also interact with the microtubule motor protein kinesin, several guanine nucleotide exchange factors, the phosphatase MKP7, Src-related protein kinases, and AKT to form multifunctional protein complexes (19).

One potential physiological role of JIP scaffold proteins is the response to metabolic stress, insulin resistance, and diabetes. Several lines of evidence support this hypothesis. First, JIP1 is required for metabolic stress-induced activation of JNK in white adipose tissue (12). Second, MLKs that interact with JIP proteins are implicated as essential components of a signaling pathway that mediates the effects of metabolic stress on JNK activation (13). Third, studies have demonstrated that the human *Jip1* gene may contribute to the development of type 2 diabetes, because a *Jip1* missense mutation was found to segregate with type 2 diabetes (26). Collectively, these data suggest that JIP proteins play a role in the cellular response to metabolic stress and the regulation of insulin resistance.

It is established that the insulin receptor substrate (IRS) group of scaffold proteins plays a central role in insulin signaling (27). Treatment of cells with insulin causes tyrosine phosphorylation of the insulin receptor, the recruitment of IRS

proteins to the insulin receptor, and the subsequent tyrosine phosphorylation of IRS proteins on multiple residues that act as docking sites for insulin-regulated signaling molecules, including phosphatidylinositol 3 kinase (27). Negative regulation of IRS proteins is implicated as a mechanism of insulin resistance and can be mediated by multiple pathways, including IRS protein phosphorylation and degradation. Thus, the mTOR/p70<sup>S6K</sup> (21, 22, 24) and the SOCS-1/3 (20) signaling pathways can regulate IRS protein degradation. Multisite phosphorylation on Ser/Thr residues can also regulate IRS protein function, including JNK phosphorylation of IRS1 on the inhibitory site Ser-307 that prevents recruitment of IRS1 to the activated insulin receptor (2).

The IRS and JIP groups of scaffold proteins may function independently to regulate JNK-dependent and insulin-dependent signal transduction. However, functional connections between these scaffold proteins have been identified. Thus, studies using *Jip1*<sup>-/-</sup> mice demonstrate that JIP1 is required for high-fat-diet-induced JNK activation in white adipose tissue, IRS1 phosphorylation on the inhibitory site Ser-307, and insulin resistance (12). These data suggest that JIP scaffold proteins function cooperatively with IRS proteins to regulate signal transduction by the insulin receptor. The purpose of this study was to examine cross talk between the JIP and IRS scaffold complexes. We demonstrate that the JIP and IRS scaffold complexes physically interact in an insulin-dependent manner and confirm that JIP proteins influence normal glucose homeostasis.

## MATERIALS AND METHODS

**Mice.** The construction of *Jip1*<sup>-/-</sup> mice (30) and *Jip2*<sup>-/-</sup> mice (17) has been described previously. Mice with a point mutation in JIP1 (Ser-59Asn) were constructed by homologous recombination in embryonic stem (ES) cells using standard methods. Briefly, a targeting vector was constructed (see Fig. 5A). This targeting vector was designed to introduce point mutations in exon 2 of the *Jip1*

\* Corresponding author. Mailing address: Howard Hughes Medical Institute, Program in Molecular Medicine, University of Massachusetts Medical School, 373 Plantation Street, Worcester, MA 01605. Phone: (508) 856-6054. Fax: (508) 856-3210. E-mail: Roger.Davis@umassmed.edu.

<sup>∇</sup> Published ahead of print on 29 June 2009.

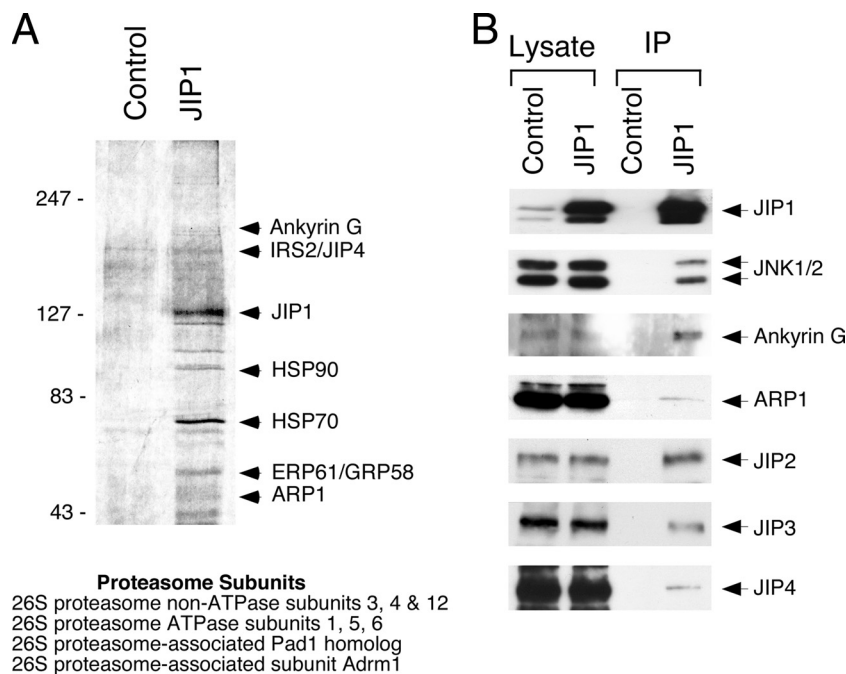


FIG. 1. Proteomic analysis of JIP protein complexes. (A) The EE monoclonal antibody was used to prepare immunoprecipitates from Rin-5F cells (Control) and from Rin-5F cells expressing EE-tagged JIP1. The immunoprecipitates were examined by sodium dodecyl sulfate-polyacrylamide gel electrophoresis. Silver-stained bands selectively present in JIP1 immunoprecipitates were excised and subjected to mass spectrometry. Sixteen different proteins were identified. Eight of these correspond to subunits of the proteasome (listed below the gel). The identities of an additional eight proteins are annotated on the gel image. (B) Coimmunoprecipitation analysis of JIP1 complex formation. EE monoclonal antibody immunoprecipitates were prepared from Rin-5F cells (Control) and Rin-5F cells expressing EE-tagged JIP1. These immunoprecipitates were probed using antibodies to JIP proteins, JNK, ankyrin G, and ARP1. Immunoblot analysis of the cell lysate (100% of the amount used for the coimmunoprecipitation) is also presented.

gene that create the Ser59Asn mutation and also a novel AseI restriction site (see Fig. 5B). TC1 ES cells (strain 129svev) were electroporated with this vector and selected with 200  $\mu\text{g}/\text{ml}$  G418 (Invitrogen) and 2  $\mu\text{M}$  ganciclovir (Syntex). Correctly targeted ES cell clones were identified by using Southern blot analysis and were injected into C57BL/6J blastocysts to create chimeric mice that were bred to obtain germ line transmission of the mutated *Jip1* allele. The floxed Neo<sup>c</sup> cassette was excised using Cre recombinase. The mice used in this study were backcrossed (10 generations) to the C57BL/6J strain (Jackson Laboratories) and were housed in a facility accredited by the American Association for Laboratory Animal Care. The Institutional Animal Care and Use Committee of the University of Massachusetts approved all studies using animals.

**Genotyping.** Genomic DNA was examined using a PCR assay to detect the wild-type and disrupted alleles of *Jip1* or *Jip2* (30). The *Jip1*<sup>S59N</sup> allele was detected using two different assays. First, Southern blot analysis of AseI-restricted genomic DNA was performed by probing with a 468-bp fragment of the *Jip1* gene that was isolated by PCR using the primers 5'-GCTCAGTAAACACACAAGGCTGGAG-3' and 5'-CCCTGGAAGATGAAGACCTCAAAG-3'. The *Jip1* and *Jip1*<sup>S59N</sup> alleles were detected as 11.9-kb and 4.9-kb bands, respectively (see Fig. 5C). Second, a PCR assay was employed using the primers 5'-ACGGAGGCATCTCTCCAATAGAGC-3', 5'-TTCTGCCTCTATCCTTGCTGGC-3', and 5'-CAGGGTGTCTTTGCCTGACTGCAGATTA-3'. The *Jip1* and *Jip1*<sup>S59N</sup> alleles were amplified to yield 1,250- and 400-bp DNA fragments, respectively (see Fig. 5D).

**Plasmids.** Mammalian expression vectors for IRS1 and IRS2 (provided by M. White), Flag- and T7-tagged JIP1 (28), and Flag- and T7-tagged JIP2 (31) have been described previously. Encoding epitope (EE)-tagged JIP1 and JIP2 were created using an in-frame insertion of nucleotides that encode the EE (EYMPME) between codons 1 and 2 of the JIP1 cDNA with a PCR-based approach. The EE-JIP1 cDNA was subcloned as a blunt-end fragment into the BamHI site of the retroviral vector pBABE-Puro.

**Blood analysis.** Insulin concentrations were measured using an enzyme-linked immunosorbent assay (ELISA) kit for rat insulin (Crystal Chem). Glucose levels were measured using a blood glucose meter (Bayer Corporation, Mishawaka, IN). Adiponec-

tin, leptin, and resistin were measured by multiplexed ELISA using LINCOplex kits (LINCO Research) assayed on a Luminex 200 instrument (LINCO Research).

**Morphology.** Histology was performed using tissue fixed in 10% formalin for 24 h, dehydrated, and embedded in paraffin. Sections (7  $\mu\text{m}$ ) were cut and stained using hematoxylin and eosin (American Master Tech Scientific). Immunohistochemistry was performed by staining tissue sections with an antibody to insulin (Dako), a biotinylated secondary antibody (BioGenex), streptavidin-conjugated horseradish peroxidase (BioGenex), and the substrate 3,3'-diaminobenzidine (Vector Laboratories), followed by brief counterstaining with Mayer's hematoxylin (Sigma). Double staining for insulin and glucagon in islets was performed using pancreatic tissue frozen in optimal cutting temperature compound (Tissue-Tek). Tissue sections (12  $\mu\text{m}$ ) were fixed in acetone, followed by staining with antibodies to insulin (Dako) and glucagon (Zymed). The primary antibodies were detected by incubation with anti-mouse or anti-rabbit immunoglobulin conjugated to Alexa Fluor 488 or 633 (Molecular Probes). The fluorescence was visualized using a Leica TCS SP2 confocal microscope equipped with a 405-nm diode laser. Analysis of fixed tissue by electron microscopy was performed using ultrathin sections mounted on copper support grids that were contrasted with lead citrate-uranyl acetate and examined on a Philips CM-10 transmission electron microscope at 80 kV accelerating voltage.

**Tissue culture.** Rin-5F, COS7, and 293T cells (American Type Culture Collection) were cultured in RPMI 1640 medium with 2 mM L-glutamine modified to contain 10 mM HEPES, 1 mM sodium pyruvate, 4.5 g/liter glucose, and 10% fetal bovine serum (Rin-5F) or Dulbecco's modified Eagle's medium supplemented with 10% fetal bovine serum (COS7 and 293T). Transient transfection assays were performed using Lipofectamine (Invitrogen). Recombinant retroviruses were prepared by transfecting 293T cells with pBABE-Puro vectors and  $\Psi$ -eco packaging DNA. Rin-5F cells were transduced with retroviruses and selected by incubation in medium containing 2.5  $\mu\text{g}/\text{ml}$  puromycin.

**Biochemical assays.** Immunoblot analysis was performed using antibodies to ankyrin G (provided by Steven Lambert, UMASS Medical School), ARP1 (Sigma), JIP1 and JIP2 (31), JIP3 (15), JIP4 (16), JNK1/2 (PharMingen), phospho-JNK (Cell Signaling), phosphotyrosine (Upstate), and  $\alpha$ -tubulin (Sigma).

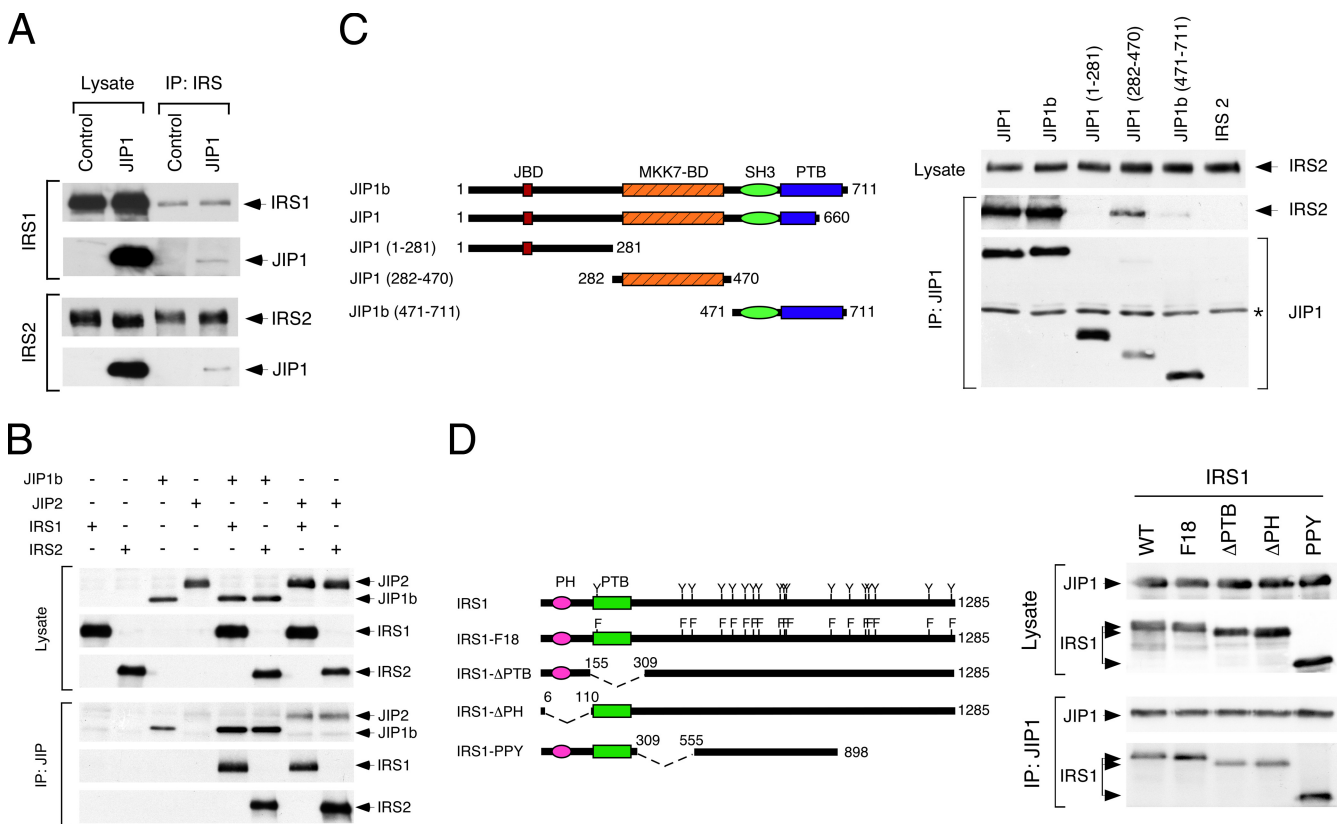


FIG. 2. Interaction of IRS and JIP proteins. (A) Immunoprecipitates of endogenous IRS1 and IRS2 were prepared from Rin-5F cells (Control) and Rin-5F cells expressing EE-tagged JIP1. These immunoprecipitates were probed using the EE monoclonal antibody and antibodies to IRS1 and IRS2. Immunoblot analysis of cell lysates (100% of the amount used for the coimmunoprecipitation) is also shown. (B) IRS proteins and T7 epitope-tagged JIP proteins were expressed in COS7 cells. The JIP proteins were immunoprecipitated using an antibody to the T7 epitope (IP). The amount of IRS and JIP proteins in the cell lysate and the immunoprecipitates was examined by immunoblot analysis using antibodies to IRS1, IRS2, and the T7 epitope tag on the JIP proteins. (C) Fragments of JIP1 with an NH<sub>2</sub>-terminal T7 epitope tag were coexpressed with IRS2 in COS7 cells. The amount of IRS2 in the cell lysate and in JIP1 (T7) immunoprecipitates (IP) was examined by immunoblot analysis using an antibody to IRS2. The amount of JIP1 in the immunoprecipitates was examined by immunoblot analysis with a T7 monoclonal antibody. The heavy chain of the immunoglobulin used for immunoprecipitation is present in every lane and is indicated by an asterisk. (D) Hemagglutinin-tagged IRS1 proteins were coexpressed with T7-tagged JIP1 in COS7 cells. The effect of IRS1 mutations was examined, including the replacement of all 18 sites of Tyr phosphorylation with Phe (F18), deletion of the PH domain (ΔPH), deletion of the PTB domain (ΔPTB), and deletion of portions of the COOH-terminal region of IRS1 (PPY). JIP1 was immunoprecipitated using a T7 monoclonal antibody. The presence of IRS1 and JIP1 in the lysate and immunoprecipitate was examined by immunoblot analysis.

JNK activity was measured in an in vitro kinase assay using c-Jun as the substrate (29). Cell lysates were prepared using buffer containing 20 mM Tris-Cl, pH 8, 137 mM NaCl, 10% glycerol, and 0.2% Triton X-100. Immunoprecipitation assays were performed by incubation of lysates with antibodies to the EE tag linked to Sepharose (Covance), Flag tag (M2, Sigma), T7 tag (Novagen), IRS1 (provided by M. White), or IRS 2 (Upstate). Coimmunoprecipitating proteins were detected by immunoblot analysis or by mass spectroscopy using matrix-assisted laser desorption ionization–quadrupole ion trap–time of flight tandem mass spectrometry analysis (J. Lesyck, Proteomics Facility, University of Massachusetts Medical School).

**RESULTS**

**Analysis of JIP1 scaffold complexes by mass spectroscopy.** We isolated JIP1 protein complexes from Rin-5F insulinoma cells by immunoprecipitation (Fig. 1A). Sodium dodecyl sulfate-polyacrylamide gel electrophoresis analysis indicated the presence of a band corresponding to the expected electrophoretic mobility of JIP1 and a number of other proteins. To identify these proteins, we performed mass spectroscopy using matrix-assisted laser desorption ionization–quadrupole ion

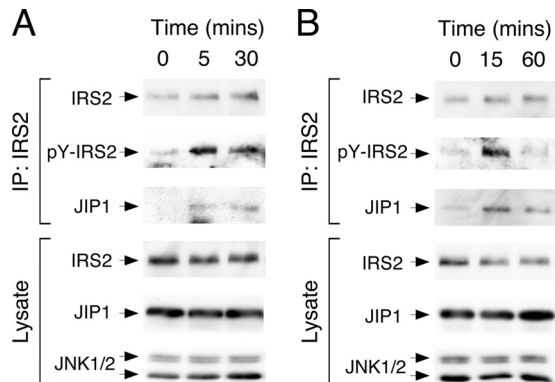


FIG. 3. Interaction of endogenous JIP1 and IRS2. Rin-5F cells were serum-starved (16 h) followed by treatment with 100 nM insulin (A) or 10% serum (B). Lysates were prepared from the cells at the indicated times, and IRS2 was isolated by immunoprecipitation. The immunoprecipitates were examined by immunoblot analysis using antibodies to IRS2, phosphotyrosine, and JIP1. The amount of IRS2, JIP1, and JNK in the cell lysates was also examined by immunoblot analysis.

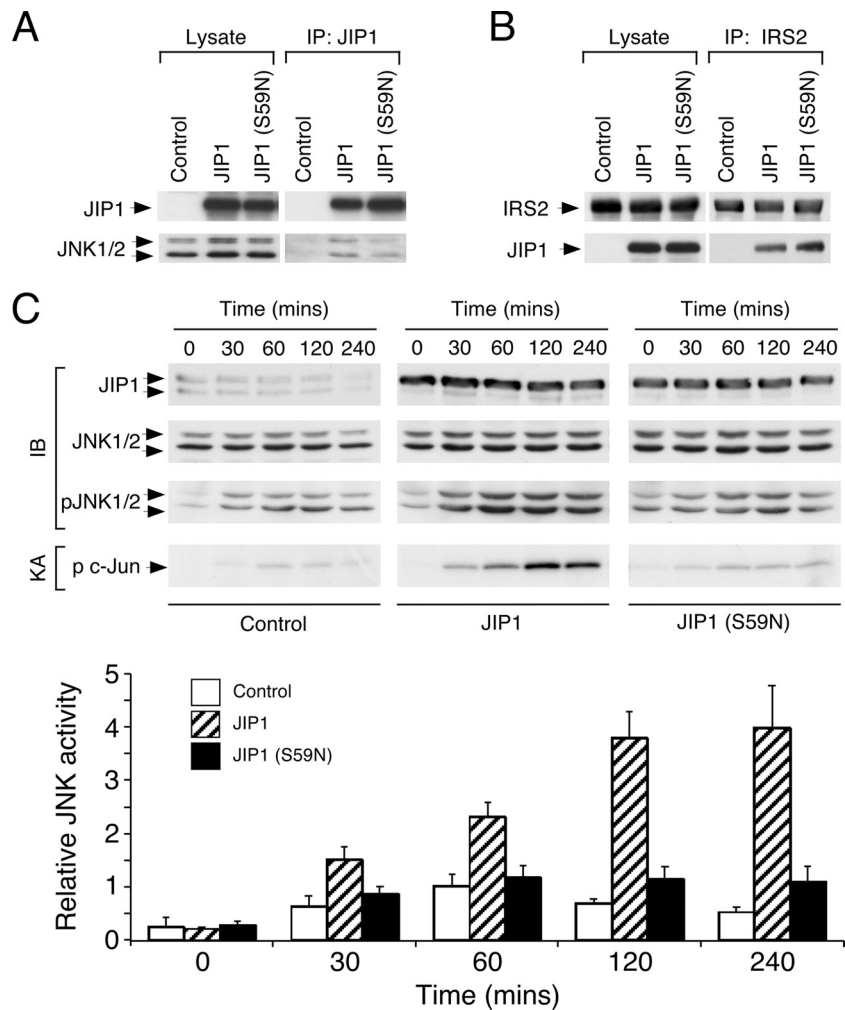


FIG. 4. The diabetes-associated polymorphism (Ser-59Asn) in JIP1 suppresses JNK activation. (A) Lysates were prepared from Rin-5F cells expressing EE-tagged JIP1 or (S59N) JIP1. Lysates and JIP1 immunoprecipitates were probed by immunoblot analysis using antibodies to JIP1 and JNK. (B) Lysates were prepared from Rin-5F cells expressing EE-tagged JIP1 or (S59N) JIP1. Cell lysates and immunoprecipitates of endogenous IRS2 were probed by immunoblot analysis using antibodies to IRS2 and JIP1. (C) Wild-type Rin-5F cells and Rin-5F cells expressing EE-tagged JIP1 or (S59N) JIP1 were exposed to UV radiation ( $60 \text{ J/m}^2$ ) and subsequently harvested at the indicated times. The amount of JIP1, JNK, and phospho-JNK was examined by immunoblot analysis (IB). JNK activity was measured in an immunocomplex kinase assay (KA) using [ $\gamma$ - $^{32}\text{P}$ ]ATP and c-Jun as substrates. An autoradiograph showing the phosphorylated c-Jun is presented, and the amount of phospho-c-Jun was quantitated by Phosphorimager analysis (mean  $\pm$  standard deviation;  $n = 4$ ). The JNK activity detected in cells expressing (S59N) JIP1 was significantly reduced compared with that of cells expressing wild-type JIP1 ( $P < 0.01$ ).

trap-time of flight tandem mass spectrometry analysis. These studies led to the identification of JIP1 and 15 additional proteins. Three of these proteins are molecular chaperones (ERP1/GRP58, HSP70, and HSP90). The presence of chaperones in JIP1 complexes was anticipated because similar molecular chaperones have been identified in other MAPK scaffold complexes (19). Eight of the identified proteins correspond to subunits of the proteasome (ATPase subunits 1, 5, and 6 and non-ATPase subunits 3, 4, and 12) and two proteasome-associated proteins (Adrm1 and Pad1 homolog). The presence of these proteasome subunits is consistent with the finding that JIP1 is degraded by the proteasome pathway (3).

Four additional proteins identified in JIP1 complexes by mass spectroscopy were not anticipated. First, a subunit of the dynactin complex (ARP1) that mediates interactions between cargo molecules and the microtubule motor protein dynein was

identified (Fig. 1A). The presence of ARP1 in JIP1 complexes was confirmed by coimmunoprecipitation-immunoblot analysis (Fig. 1B). Previous studies have established that JIP1 interacts with the light chain of the microtubule motor protein kinesin 1 (25, 30). Together, these findings suggest that JIP1 trafficking on microtubules may be mediated by both kinesin and dynein motor proteins. Second, the cytoskeletal protein ankyrin G was identified in JIP1 complexes (Fig. 1A), and this was confirmed by coimmunoprecipitation-immunoblot analysis (Fig. 1B). Since ankyrin G is localized to the initial segment of axons and is implicated in axonal protein recruitment (14), the interaction of JIP1 with ankyrin G may account for the localization of JIP1 in axonal projections during the early phase of neuronal differentiation (7). Finally, two different scaffold proteins (IRS2 and JIP4) were found in JIP1 immunoprecipitates (Fig. 1A). Coimmunoprecipitation analysis confirmed that JIP4 was

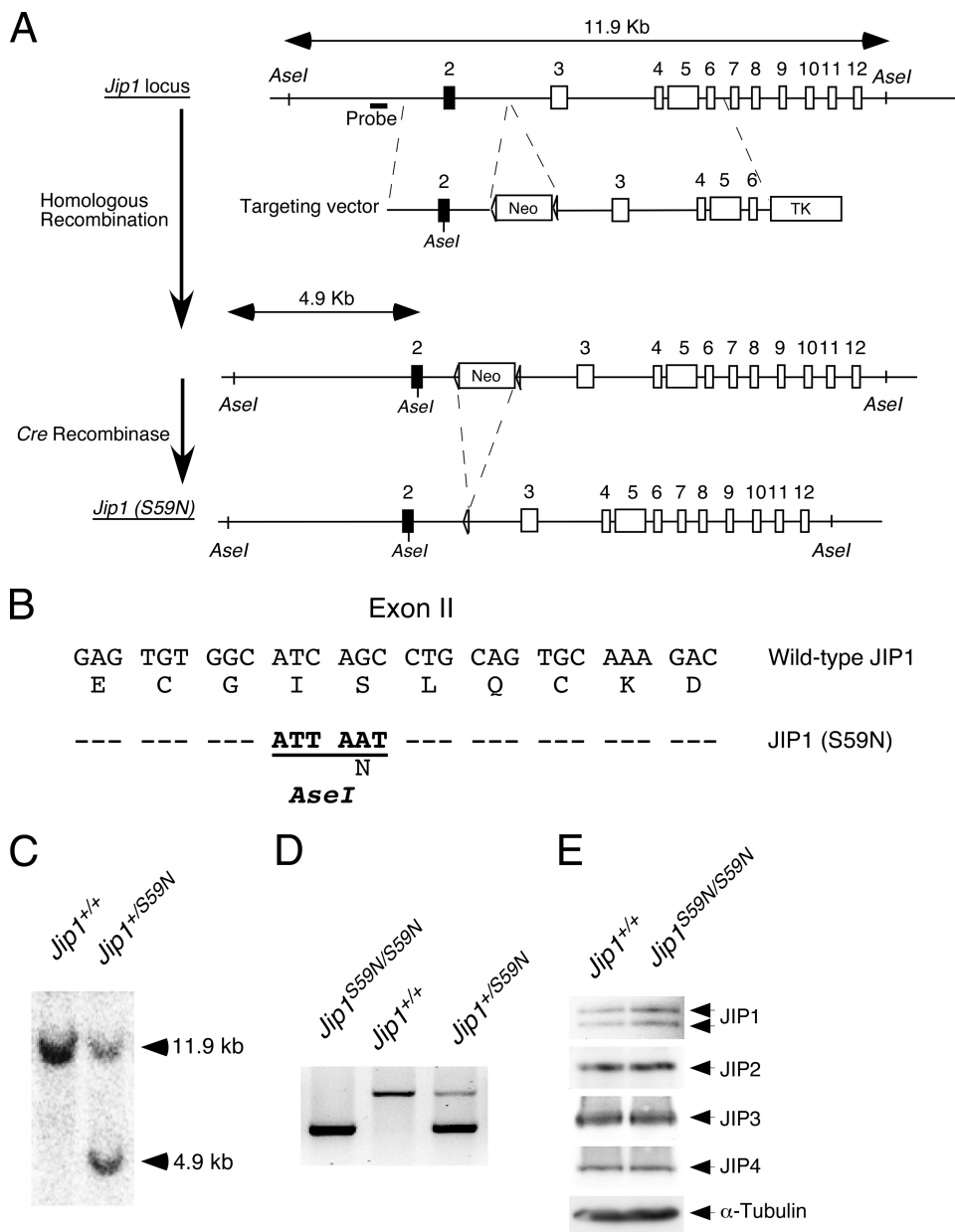


FIG. 5. Creation of mice with the germ line point mutation Ser-59Asn in the *Jip1* gene. (A to B) A targeting vector was designed to replace Ser-59 with Asn and to introduce silent mutations that create an *AseI* site in exon II of the *Jip1* gene by homologous recombination in ES cells. The floxed *Neo<sup>r</sup>* cassette used for selection was deleted using Cre recombinase. (C) Genomic DNA isolated from wild-type and mutant ES cells was digested with *AseI* and examined by Southern blot analysis to confirm the correct targeting of the *Jip1* gene. (D) Genomic DNA isolated from wild-type (*Jip1<sup>+/+</sup>*), heterozygous (*Jip1<sup>+/S59N</sup>*), and homozygous (*Jip1<sup>S59N/S59N</sup>*) mice was examined by PCR analysis. (E) Brain lysates from *Jip1<sup>+/+</sup>* and *Jip1<sup>S59N/S59N</sup>* mice were examined by immunoblot analysis using antibodies to JIP1, JIP2, JIP3, JIP4, and  $\alpha$ -tubulin.

present in JIP1 complexes but also demonstrated the presence of both JIP2 and JIP3 (Fig. 1B).

**The JIP1 scaffold complex interacts with IRS proteins.** Proteomic analysis of JIP1 scaffold complexes led to the identification of IRS2 (Fig. 1). To test the interaction of JIP1 with IRS proteins, we immunoprecipitated endogenous IRS1 and IRS2 from lysates prepared from Rin5F cells and probed these immunoprecipitates for the presence of JIP1. This analysis demonstrated that JIP1 coimmunoprecipitated with both IRS1 and IRS2. Transfection assays confirmed the coimmunoprecipita-

tion of JIP1 with IRS1 and IRS2 (Fig. 2B) and also demonstrated that the JIP1-related protein JIP2 coimmunoprecipitated with IRS1 and IRS2 (Fig. 2B). Both JIP1 and the splice variant JIP1b were able to interact with IRS2 (Fig. 2C). Deletion analysis of JIP1b demonstrated that the NH<sub>2</sub> terminus (residues 1 to 281) and COOH terminus (residues 471 to 711) did not interact with IRS2, but the central region of JIP1b (residues 282 to 470) was sufficient for binding IRS2 (Fig. 2C). Mutational analysis of IRS1 demonstrated that neither the PH and PTB domains nor the 18 sites of Tyr phosphorylation of

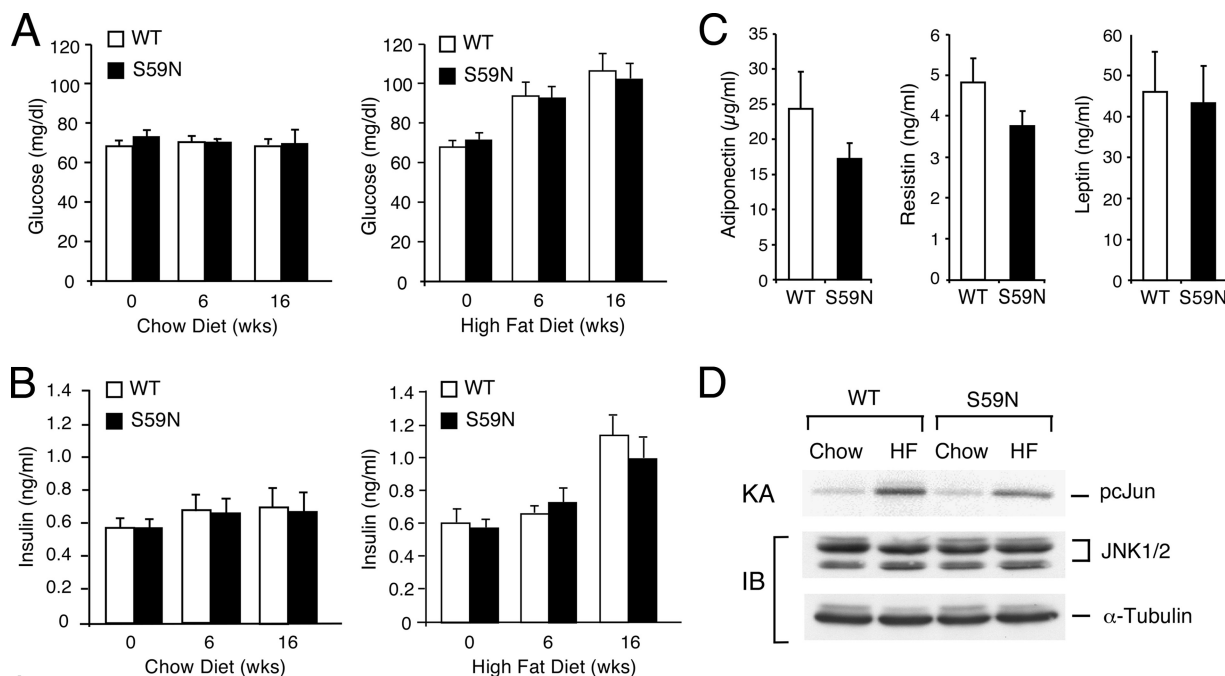


FIG. 6. Metabolic effect of the *Jip1*<sup>S59N</sup> mutation on the response to feeding a high-fat diet. Male *Jip1*<sup>+/+</sup> (WT) and *Jip1*<sup>S59N/S59N</sup> (S59N) mice were fed a standard chow diet (control) or a high-fat (HF) diet for 0, 6, or 16 weeks. (A to B) The mice were fasted overnight, and the plasma concentrations of glucose (A) and insulin (B) were measured (mean  $\pm$  standard deviation [SD];  $n = 12$ ). (C) The amount of plasma adiponectin, resistin, and leptin after 16 weeks on the diet was measured by multiplexed ELISA assays (mean  $\pm$  SD;  $n = 12$ ). (D) The activity of JNK in epididymal fat pads of the mice after 16 weeks on the control or HF diet was measured by using the immunocomplex kinase assay (KA) using [ $\gamma$ -<sup>32</sup>P]ATP and c-Jun as the substrates. The amount of JNK and  $\alpha$ -tubulin in the cell lysate was examined by immunoblot analysis.

IRS1 were required for the interaction of IRS1 with JIP1 (Fig. 2D). However, a truncated IRS1 protein (IRS1-PPY) was sufficient for binding JIP1 (Fig. 2D).

**Insulin regulates the interaction of JIP and IRS scaffold proteins.** Coimmunoprecipitation analysis demonstrated an interaction between a fraction of the total JIP and IRS molecules within the cell (Fig. 2). To test whether this interaction was regulated by hormonal stimulation, we examined the effect of treatment of cells with insulin on the coimmunoprecipitation of JIP1 with IRS2 (Fig. 3). We found that the treatment of cells with insulin caused no change in the expression of JIP1, IRS2, or JNK1/2. However, when endogenous IRS2 was immunoprecipitated from lysates prepared from insulin-stimulated cells, the amount of coimmunoprecipitated JIP1 was increased (Fig. 3A). Similar results were obtained when the cells were treated with serum (Fig. 3B). These observations suggest that JIP/IRS complexes may be dynamically regulated within cells.

**Mutational analysis of JIP1 in vivo.** JIP1 has been implicated in type 2 diabetes because *Jip1*<sup>-/-</sup> mice exhibit defects in high-fat-diet-induced JNK activation and insulin resistance (12). Furthermore, in studies of humans, a missense mutation in the coding region of the *Jip1* gene that replaces Ser-59 with an Asn residue was found to segregate with type 2 diabetes, demonstrating that the *Jip1* gene may contribute to type 2 diabetes (26). This mutation may influence the function of JIP1 (1, 3, 26). To test this hypothesis, we immunoprecipitated wild-type and Ser-59Asn JIP1 from Rin5F insulinoma cells and examined the amount of associated endogenous JNK and IRS2 by immunoblot analysis. This analysis demonstrated that the

Ser-59Asn mutation did not affect the binding of JIP1 to JNK or IRS2 (Fig. 4A and B). Nevertheless, the Ser-59Asn mutation did cause defects in JIP1 protein function. Thus, expression of wild-type JIP1, but not Ser-59Asn JIP1, was found to cause increased stress-induced activation of JNK (Fig. 4C). This effect of the Ser-59Asn mutation was detected when JNK activation was monitored by *in vitro* protein kinase assays and by immunoblot analysis using a phospho-JNK antibody (Fig. 4C).

The segregation of the Ser-59Asn mutation with human type 2 diabetes (26) and the finding that this mutation alters the biochemical properties of JIP1 (Fig. 4) suggested that the Ser-59Asn JIP1 protein warranted further study. We therefore created mice on the C57BL/6J strain background with a germ line mutation in the *Jip1* gene at codon 59 (Fig. 5A to D). Heterozygous matings resulted in progeny with the expected Mendelian ratios of wild-type, homozygous, and heterozygous mice. The homozygous *Jip1*<sup>S59N/S59N</sup> mice were found to be viable and fertile. Immunoblot analysis demonstrated that similar amounts of JIP1 protein were detected in wild-type and *Jip1*<sup>S59N/S59N</sup> mice (Fig. 5E). No compensatory changes in the expression of JIP2, JIP3, or JIP4 were detected (Fig. 5E). To test whether the Ser-59Asn mutation might alter the response of mice being fed a high-fat diet, we examined cohorts of littermate wild-type and *Jip1*<sup>S59N/S59N</sup> male mice fed either a standard chow diet or a high-fat diet for 16 weeks. Both the wild-type and mutant mice gained similar body mass and adiposity (data not shown) together with development of mild fasting hyperglycemia (Fig. 6A) and hyperinsulinemia (Fig.

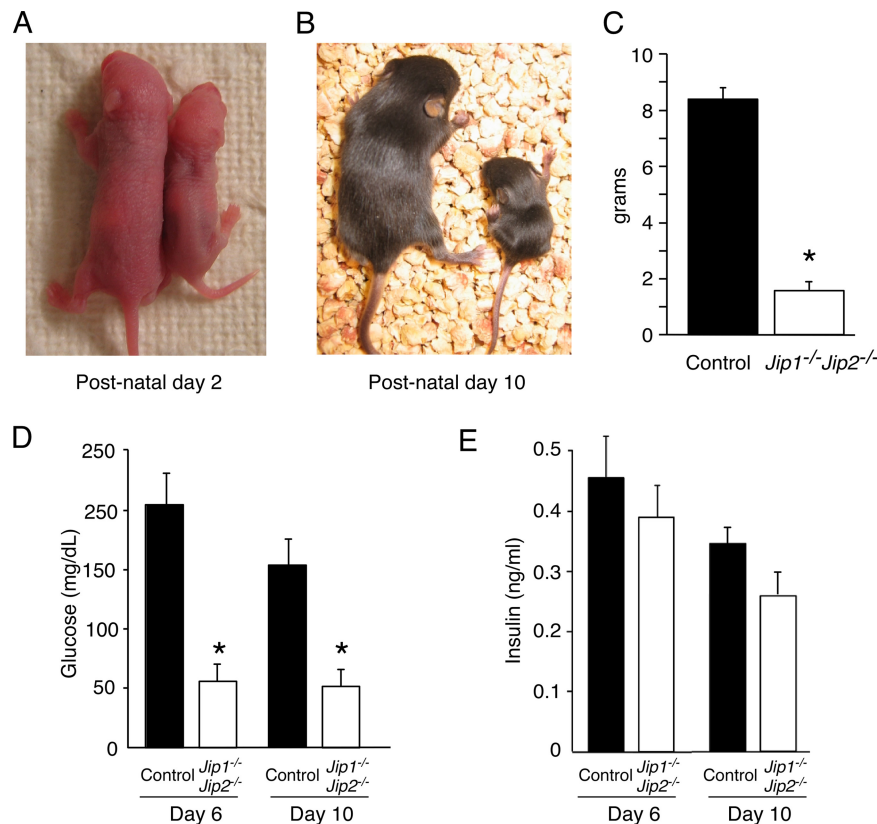


FIG. 7. *Jip1/2* compound mutant mice exhibit severe growth retardation. (A and B) Littermate *Jip1<sup>-/-</sup> Jip2<sup>-/-</sup>* mice (left) and control (*Jip1<sup>-/-</sup> Jip2<sup>+/+</sup>*) mice (right) at postnatal day 2 and day 10 are illustrated. (C) The body masses of littermate *Jip1<sup>-/-</sup> Jip2<sup>-/-</sup>* mice and control (*Jip1<sup>-/-</sup> Jip2<sup>+/+</sup>*) mice at postnatal day 10 are presented (mean  $\pm$  standard deviation [SD];  $n = 6$ ). The masses of the *Jip1<sup>-/-</sup> Jip2<sup>-/-</sup>* mice were significantly less than those of the control mice. \*,  $P < 0.001$ . (D and E) Blood collected from wild-type and *Jip1<sup>-/-</sup> Jip2<sup>-/-</sup>* mice was used to measure the amount of glucose (D) and insulin (E). The data presented are the mean  $\pm$  SD ( $n = 10$ ). Significant differences between the *Jip1<sup>-/-</sup> Jip2<sup>-/-</sup>* mice and control mice are indicated. \*,  $P < 0.01$ .

6B). Similarly, no significant differences in glucose tolerance and insulin tolerance tests (data not shown) and the blood concentration of the adipokines adiponectin, resistin, and leptin were detected between wild-type and *Jip1<sup>S59N/S59N</sup>* mice (Fig. 6C). Nevertheless, feeding a high-fat diet caused a reproducible, but modest, reduction in JNK activation in *Jip1<sup>S59N/S59N</sup>* mice compared with wild-type mice (Fig. 6D). Thus, the Ser-59Asn mutation in JIP1 causes marked changes in stress-induced JNK activation in transfected cultured cells (Fig. 4), but this mutation in the endogenous *Jip1* gene caused only a small change in obesity-induced JNK activation (Fig. 6D). The small size of the decrease in JNK activation in vivo may account for our failure to detect metabolic consequences of the Ser-59Asn mutation in mice. Together, these data indicate that in a C57BL/6J genetic background, the Ser-59Asn mutation in JIP1, by itself, does not increase the susceptibility of mice to diet-induced obesity and insulin resistance.

**Redundant functions of JIP1 and JIP2.** The absence of a detected diabetes-related phenotype in *Jip1<sup>S59N/S59N</sup>* mice was unexpected (Fig. 6). One explanation for this finding is that the altered function of the Ser-59Asn JIP1 protein is compensated by the expression of other JIP family proteins in mice. Indeed, the JIP2 scaffold protein shares the same domain structure as JIP1 (19). In contrast, the JIP3 and JIP4 scaffold proteins are

structurally distinct proteins (19). These considerations suggest the possibility that there are functional redundancies between the JIP1 and JIP2 scaffold proteins. Indeed, both JIP1 and JIP2 scaffold proteins form complexes with IRS1 and IRS2 (Fig. 2B). To test this hypothesis, we created compound mutant mice that lack expression of both JIP1 and JIP2 (Fig. 7A to C). The *Jip1<sup>-/-</sup> Jip2<sup>-/-</sup>* mice exhibited severe growth retardation compared with littermate control mice and died within 2 weeks after birth. This phenotype was not observed in studies of *Jip1<sup>S59N/S59N</sup> Jip2<sup>-/-</sup>* mice, consistent with the conclusion that the Ser-59Asn JIP1 mutation causes only a partial loss JIP1 function. Interestingly, a comparison of *Jip1<sup>-/-</sup> Jip2<sup>-/-</sup>* mice to littermate control mice demonstrated that the mutant mice were hypoglycemic (Fig. 7D). It is possible that the ataxic phenotype of *Jip1<sup>-/-</sup> Jip2<sup>-/-</sup>* mice (17) may disrupt feeding behavior and therefore contribute to the hypoglycemia. Nevertheless, our analysis indicates that JIP proteins in mice are required for normal glucose homeostasis.

We have previously reported that JIP1-deficient mice exhibit a major defect in IRS1 phosphorylation on Ser-307 in white adipose tissue (12). White adipose tissue expresses JIP1, but not JIP2. In contrast, brown adipose tissue expresses both JIP1 and JIP2. We therefore examined the effect of JIP1 deficiency and JIP1/2 deficiency on IRS1 phosphorylation in brown fat

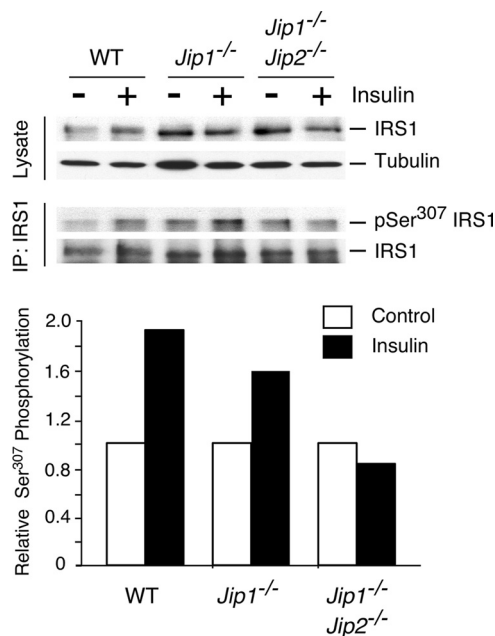


FIG. 8. Defects in the phosphorylation of IRS1 on Ser-307 in *Jip1/2* compound mutant mice. Wild-type mice, *Jip1*<sup>-/-</sup> mice, and *Jip1*<sup>-/-</sup> *Jip2*<sup>-/-</sup> mice (postnatal day 1) were treated without and with 1.5 U/kg insulin by intraperitoneal injection. Extracts prepared from brown fat were examined by immunoblot analysis using antibodies to IRS1 and  $\alpha$ -tubulin. IRS1 immunoprecipitates prepared from the cell lysate were probed with antibodies to IRS1 and phospho-Ser-307 IRS1. Densitometric analysis of immunoblots was employed to quantitate the effect of insulin to increase the phosphorylation of IRS1 on Ser-307.

tissue (Fig. 8). We found that JIP1 deficiency partially decreased, and that JIP1/2-deficiency blocked, insulin-stimulated IRS1 Ser-307 phosphorylation. These data indicate that JIP1 and JIP2 can function cooperatively to induce IRS1 Ser-307 phosphorylation.

The JIP1 and JIP2 scaffold proteins have been reported to be critical for the function and viability of pancreatic islets (5, 6, 9, 18). However, histological and immunocytochemical examination of pancreatic sections from *Jip1*<sup>-/-</sup> *Jip2*<sup>-/-</sup> mice showed no obvious defect in islet morphology or in the levels of insulin in  $\beta$  cells or glucagon in  $\alpha$  cells (Fig. 9A to C). These data demonstrate that, despite previous reports indicating an important role of JIPs in insulin expression and  $\beta$ -cell viability (5, 6, 9, 18), the JIP1 and JIP2 proteins are not essential for these processes. Nevertheless, detailed analysis of the pancreas using electron microscopy did demonstrate that the  $\beta$  cells of *Jip1*<sup>-/-</sup> *Jip2*<sup>-/-</sup> mice contained fewer exocytotic vesicles than those of control mice (Fig. 9D). However, no significant difference in blood insulin concentration was detected between control and *Jip1*<sup>-/-</sup> *Jip2*<sup>-/-</sup> mice (Fig. 7E).

## DISCUSSION

The IRS and JIP scaffold proteins are implicated in the regulation of the insulin and JNK signaling pathways, respectively. Here we identify evidence of cross talk between these two scaffold complexes. A proteomic mass spectroscopy approach and coimmunoprecipitation analysis demonstrated that

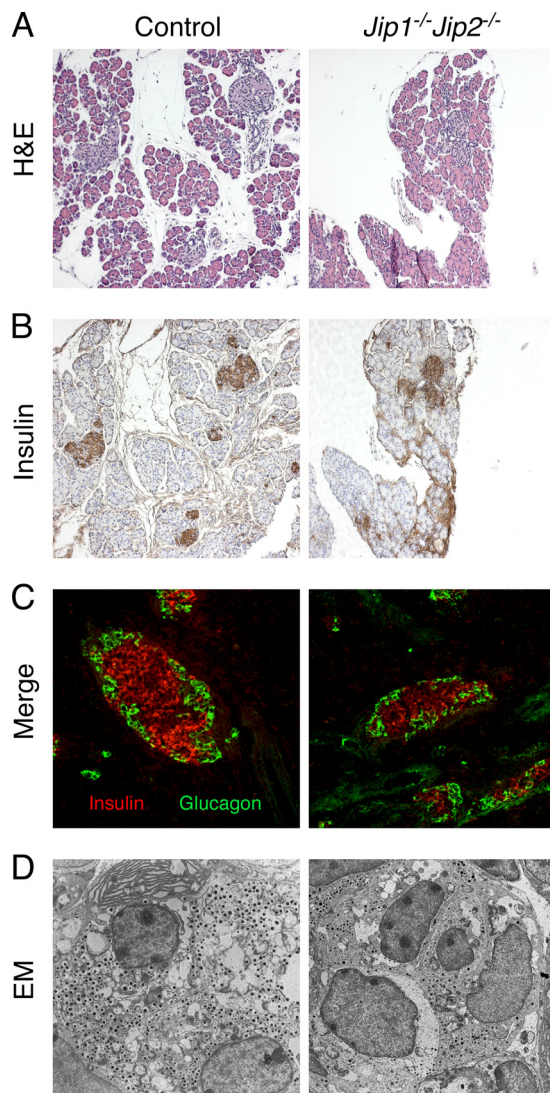


FIG. 9. Pancreatic morphology of *Jip1/2* compound mutant mice. (A to C) Sections of the pancreases from 7-day-old wild-type and *Jip1*<sup>-/-</sup> *Jip2*<sup>-/-</sup> mice were stained with hematoxylin and eosin (A) or with antibodies to insulin (B) or to insulin and glucagon (C). (D) The morphology of pancreatic  $\beta$  cells was examined by using electron microscopy.

JIP1 and JIP2 protein complexes interact with IRS1 and IRS2 complexes (Fig. 1 and 2). Indeed, this interaction is increased in cells treated with insulin (Fig. 3). The physiological significance of this finding is most likely related to the role of JNK in the regulation of insulin resistance (11) by mechanisms that include the phosphorylation of IRS1 on the negative regulatory site Ser-307 (2).

During diet-induced obesity, JNK is activated by a signaling pathway that is mediated by MLKs (13) that interact with JIP scaffold proteins (12). Indeed, JIP scaffold proteins may assemble a JNK signaling module composed of a MAPK kinase (one or more members of the MLK protein family), the MAPK kinase MKK7, and JNK (28). Interestingly, high-fat-diet-induced JNK activation in vivo is severely attenuated in *Mlk3*<sup>-/-</sup> and *Jip1*<sup>-/-</sup> mice (12, 13). This requirement of JIP1



signaling complexes for high-fat-diet-induced JNK activation provides an explanation for the finding that both *Mlk3*<sup>-/-</sup> and *Jip1*<sup>-/-</sup> mice exhibit marked defects in the phosphorylation of the IRS1 scaffold protein on the negative regulatory site Ser-307 (12, 13). The interaction of JIP and IRS signaling complexes suggests that JIP proteins may locally activate JNK and also target JNK toward IRS protein phosphorylation.

The concept that scaffold molecules can increase signaling specificity by locally activating specific signaling pathways is well established (23). In addition, examples of substrate tethering by scaffold proteins have been described previously, including the interaction of AKAP scaffold proteins with glutamate receptors (4). The interaction of IRS and JIP scaffold complexes provides another example of localized signaling and substrate targeting. A critical test of this hypothesis will be the analysis of mice with a germ line mutation in the *Jip1* or *Jip2* gene that does not affect JIP-mediated JNK activation but does disrupt the interaction of JIP1/2 with IRS1/2 proteins. The creation of such mice represents an important goal for future studies.

The link between JIP proteins and the insulin receptor signaling pathway that we have identified is intriguing. The data suggest that JIP proteins may influence insulin signaling in disease. Indeed, it has been reported that the Ser-59Asn mutation in the human *Jip1* gene segregates with type 2 diabetes (26), and JIP1 has been implicated as a protein that is critical for the normal function of pancreatic islets, including insulin gene expression and  $\beta$ -cell viability (5, 6, 9, 18). Furthermore, biochemical analysis demonstrated that the Ser-59Asn mutation has a profound effect on JIP1 protein function, including an altered ability to activate JNK (Fig. 4C). These data strongly implicate the mutated human *Jip1* allele in disease. To test this hypothesis, we generated mice with a germ line mutation in the *Jip1* gene that encodes Asn rather than Ser at codon 59. We found that this mutation did not predispose C57BL/6J mice to type 2 diabetes when they were fed either chow or a high-fat diet (Fig. 6). Our failure to detect a diabetes-related phenotype in Ser-59Asn JIP1 mice may represent a difference between mouse and human physiology. However, it may be significant that a large fraction of the diabetic patients with the mutant *Jip1* allele were also carriers of a *Pdx1* (*Ipf1*) mutation (26) that has been previously associated with a late-onset form of diabetes (10). Thus, the Ser-59Asn *Jip1* mutation in humans may be particularly important in diabetes pathogenesis in patients with increased diabetes susceptibility, including *Pdx1* (*Ipf1*) mutations.

Although the Ser-59Asn mutation in JIP1 may not be sufficient, by itself, to cause obvious disease, it is likely that JIP1 proteins contribute to some aspects of metabolic syndrome. Indeed, JIP1-deficient mice exhibit marked defects in obesity-induced activation of the JNK signaling pathway (12). Since the structurally related protein JIP2 also interacts with IRS proteins (Fig. 2), it was possible that the JIP1 and JIP2 proteins may have partially redundant functions. Indeed, we found that the JIP1/2-deficient mice exhibited a severe growth retardation phenotype, hypoglycemia, and early death (Fig. 7). This phenotype was not observed in *Jip1*<sup>-/-</sup> mice (30) or *Jip2*<sup>-/-</sup> mice (17). These data confirm that the JIP1 and JIP2 proteins do exhibit partially redundant functions and that these JIP proteins are essential for normal glucose homeostasis.

## ACKNOWLEDGMENTS

We thank Morris White and Steven Lambert for providing essential reagents, John Leszyck for mass spectroscopy, Stephen Jones for blastocyst injections, Linda Evangelista for ES cell culture, Guadalupe Sabio for assistance with Luminex assays, Heather Collins for plasma insulin measurements, Beth Doran, Jian-Hua Liu, and Judith Reilly for expert technical assistance, and Kathy Gemme for administrative assistance.

These studies were supported by a grant from the National Institutes of Health. Core facilities used by these studies were supported by the NIDDK Diabetes and Endocrinology Center (P30 DK 32520) at the University of Massachusetts. R.A.F. and R.J.D. are investigators of the Howard Hughes Medical Institute.

## REFERENCES

1. Abe, H., K. Murao, H. Imachi, W. M. Cao, X. Yu, K. Yoshida, N. C. Wong, M. A. Shupnik, J. A. Haefliger, G. Waeber, and T. Ishida. 2004. Thyrotropin-releasing hormone-stimulated thyrotropin expression involves islet-brain-1/c-Jun N-terminal kinase interacting protein-1. *Endocrinology* **145**:5623–5628.
2. Aguirre, V., T. Uchida, L. Yenush, R. Davis, and M. F. White. 2000. The c-Jun NH(2)-terminal kinase promotes insulin resistance during association with insulin receptor substrate-1 and phosphorylation of Ser(307). *J. Biol. Chem.* **275**:9047–9054.
3. Allaman-Pillet, N., J. Stirling, A. Oberson, R. Roduit, S. Negri, C. Sauser, P. Nicod, J. S. Beckmann, D. F. Schorderet, T. Mandrup-Poulsen, and C. Bonny. 2003. Calcium- and proteasome-dependent degradation of the JNK scaffold protein islet-brain 1. *J. Biol. Chem.* **278**:48720–48726.
4. Bauman, A. L., A. S. Goehring, and J. D. Scott. 2004. Orchestration of synaptic plasticity through AKAP signaling complexes. *Neuropharmacology* **46**:299–310.
5. Bonny, C., P. Nicod, and G. Waeber. 1998. IB1, a JIP-1-related nuclear protein present in insulin-secreting cells. *J. Biol. Chem.* **273**:1843–1846.
6. Bonny, C., A. Oberson, M. Steinmann, D. F. Schorderet, P. Nicod, and G. Waeber. 2000. IB1 reduces cytokine-induced apoptosis of insulin-secreting cells. *J. Biol. Chem.* **275**:16466–16472.
7. Dajas-Bailador, F., E. V. Jones, and A. J. Whitmarsh. 2008. The JIP1 scaffold protein regulates axonal development in cortical neurons. *Curr. Biol.* **18**:221–226.
8. Dickens, M., J. S. Rogers, J. Cavanagh, A. Raitano, Z. Xia, J. R. Halpern, M. E. Greenberg, C. L. Sawyers, and R. J. Davis. 1997. A cytoplasmic inhibitor of the JNK signal transduction pathway. *Science* **277**:693–696.
9. Haefliger, J. A., T. Tawadros, L. Meylan, S. L. Gurun, M. E. Roehrich, D. Martin, B. Thorens, and G. Waeber. 2003. The scaffold protein IB1/JIP-1 is a critical mediator of cytokine-induced apoptosis in pancreatic beta cells. *J. Cell Sci.* **116**:1463–1469.
10. Hani, E. H., D. A. Stoffers, J. C. Chevre, E. Durand, V. Stanojevic, C. Dina, J. F. Habener, and P. Froguel. 1999. Defective mutations in the insulin promoter factor-1 (IPF-1) gene in late-onset type 2 diabetes mellitus. *J. Clin. Invest.* **104**:R41–R48.
11. Hirosumi, J., G. Tuncman, L. Chang, C. Z. Gorgun, K. T. Uysal, K. Maeda, M. Karin, and G. S. Hotamisligil. 2002. A central role for JNK in obesity and insulin resistance. *Nature* **420**:333–336.
12. Jaeschke, A., M. P. Czech, and R. J. Davis. 2004. An essential role of the JIP1 scaffold protein for JNK activation in adipose tissue. *Genes Dev.* **18**:1976–1980.
13. Jaeschke, A., and R. J. Davis. 2007. Metabolic stress signaling mediated by mixed-lineage kinases. *Mol. Cell* **27**:498–508.
14. Jenkins, S. M., and V. Bennett. 2001. Ankyrin-G coordinates assembly of the spectrin-based membrane skeleton, voltage-gated sodium channels, and L1 CAMs at Purkinje neuron initial segments. *J. Cell Biol.* **155**:739–746.
15. Kelkar, N., S. Gupta, M. Dickens, and R. J. Davis. 2000. Interaction of a mitogen-activated protein kinase signaling module with the neuronal protein JIP3. *Mol. Cell Biol.* **20**:1030–1043.
16. Kelkar, N., C. L. Standen, and R. J. Davis. 2005. Role of the JIP4 scaffold protein in the regulation of mitogen-activated protein kinase signaling pathways. *Mol. Cell Biol.* **25**:2733–2743.
17. Kennedy, N. J., G. Martin, A. G. Ehrhardt, J. Cavanagh-Kyros, C. Y. Kuan, P. Rakic, R. A. Flavell, S. N. Treisman, and R. J. Davis. 2007. Requirement of JIP scaffold proteins for NMDA-mediated signal transduction. *Genes Dev.* **21**:2336–2346.
18. Ling, Z., M. Van De Castele, J. Dong, H. Heimberg, J. A. Haefliger, G. Waeber, F. Schuit, and D. Pipeleers. 2003. Variations in IB1/JIP1 expression regulate susceptibility of beta-cells to cytokine-induced apoptosis irrespective of C-Jun NH(2)-terminal kinase signaling. *Diabetes* **52**:2497–2502.
19. Morrison, D. K., and R. J. Davis. 2003. Regulation of MAP kinase signaling modules by scaffold proteins in mammals. *Annu. Rev. Cell Dev. Biol.* **19**:91–118.
20. Rui, L., M. Yuan, D. Frantz, S. Shoelson, and M. F. White. 2002. SOCS-1

- and SOCS-3 block insulin signaling by ubiquitin-mediated degradation of IRS1 and IRS2. *J. Biol. Chem.* **277**:42394–42398.
21. **Shah, O. J., and T. Hunter.** 2006. Turnover of the active fraction of IRS1 involves raptor-mTOR- and S6K1-dependent serine phosphorylation in cell culture models of tuberous sclerosis. *Mol. Cell. Biol.* **26**:6425–6434.
  22. **Shah, O. J., Z. Wang, and T. Hunter.** 2004. Inappropriate activation of the TSC/Rheb/mTOR/S6K cassette induces IRS1/2 depletion, insulin resistance, and cell survival deficiencies. *Curr. Biol.* **14**:1650–1656.
  23. **Smith, F. D., L. K. Langeberg, and J. D. Scott.** 2006. The where's and when's of kinase anchoring. *Trends Biochem. Sci.* **31**:316–323.
  24. **Um, S. H., F. Frigerio, M. Watanabe, F. Picard, M. Joaquin, M. Sticker, S. Fumagalli, P. R. Allegrini, S. C. Kozma, J. Auwerx, and G. Thomas.** 2004. Absence of S6K1 protects against age- and diet-induced obesity while enhancing insulin sensitivity. *Nature* **431**:200–205.
  25. **Verhey, K. J., D. Meyer, R. Deehan, J. Blenis, B. J. Schnapp, T. A. Rapoport, and B. Margolis.** 2001. Cargo of kinesin identified as JIP scaffolding proteins and associated signaling molecules. *J. Cell Biol.* **152**:959–970.
  26. **Waeber, G., J. Delplanque, C. Bonny, V. Mooser, M. Steinmann, C. Widmann, A. Maillard, J. Miklossy, C. Dina, E. H. Hani, N. Vionnet, P. Nicod, P. Boutin, and P. Froguel.** 2000. The gene MAPK8IP1, encoding islet-brain-1, is a candidate for type 2 diabetes. *Nat. Genet.* **24**:291–295.
  27. **White, M. F.** 2006. Regulating insulin signaling and beta-cell function through IRS proteins. *Can. J. Physiol. Pharmacol.* **84**:725–737.
  28. **Whitmarsh, A. J., J. Cavanagh, C. Tournier, J. Yasuda, and R. J. Davis.** 1998. A mammalian scaffold complex that selectively mediates MAP kinase activation. *Science* **281**:1671–1674.
  29. **Whitmarsh, A. J., and R. J. Davis.** 2001. Analyzing JNK and p38 mitogen-activated protein kinase activity. *Methods Enzymol.* **332**:319–336.
  30. **Whitmarsh, A. J., C. Y. Kuan, N. J. Kennedy, N. Kelkar, T. F. Haydar, J. P. Mordes, M. Appel, A. A. Rossini, S. N. Jones, R. A. Flavell, P. Rakic, and R. J. Davis.** 2001. Requirement of the JIP1 scaffold protein for stress-induced JNK activation. *Genes Dev.* **15**:2421–2432.
  31. **Yasuda, J., A. J. Whitmarsh, J. Cavanagh, M. Sharma, and R. J. Davis.** 1999. The JIP group of mitogen-activated protein kinase scaffold proteins. *Mol. Cell. Biol.* **19**:7245–7254.